ARTICLE IN PRESS

Communications Earth & Environment https://doi.org/10.1038/s43247-026-03522-y

Article in Press

Expansion of greenhouses alters water use and underscores the need to balance food and water security in Mediterranean catchments

Received: 9 September 2025

Accepted: 7 April 2026

Cite this article as: la Cecilia, D., Paniconi, C., Mercogliano, P. *et al.* Expansion of greenhouses alters water use and underscores the need to balance food and water security in Mediterranean catchments. *Commun Earth Environ* (2026). https://doi.org/10.1038/s43247-026-03522-y

Daniele la Cecilia, Claudio Paniconi, Paola Mercogliano & Matteo Camporese

We are providing an unedited version of this manuscript to give early access to its findings. Before final publication, the manuscript will undergo further editing. Please note there may be errors present which affect the content, and all legal disclaimers apply.

If this paper is publishing under a Transparent Peer Review model then Peer Review reports will publish with the final article.

ARTICLE IN PRESS

© The Author(s) 2026. **Open Access** This article is licensed under a Creative Commons Attribution 4.0 International License, which permits use, sharing, adaptation, distribution and reproduction in any medium or format, as long as you give appropriate credit to the original author(s) and the source, provide a link to the Creative Commons licence, and indicate if changes were made. The images or other third party material in this article are included in the article's Creative Commons licence, unless indicated otherwise in a credit line to the material. If material is not included in the article's Creative Commons licence and your intended use is not permitted by statutory regulation or exceeds the permitted use, you will need to obtain permission directly from the copyright holder. To view a copy of this licence, visit http://creativecommons.org/licenses/by/4.0/.

ARTICLE IN PRESS

Expansion of greenhouses alters water use and underscores the need to balance food and water security in Mediterranean catchments

Daniele la Cecilia[1,2], Claudio Paniconi[3], Paola Mercogliano[4] and Matteo Camporese[1]

1. Department of Civil, Environmental and Architectural Engineering, University of Padua, Padua, Italy
2. Department of Engineering Enzo Ferrari, University of Modena and Reggio Emilia, Modena, Italy
3. Centre Eau Terre Environnement, Institut national de la recherche scientifique, Quebec City, Canada
4. CMCC Foundation - Euro-Mediterranean Center on Climate Change, Caserta, Italy

Corresponding author: Dr. Daniele la Cecilia
Department of Civil, Environmental and Architectural Engineering
University of Padua
35131 Padua, Italy
daniele.lacecilia@unipd.it

Corresponding author: Prof. Matteo Camporese
Department of Civil, Environmental and Architectural Engineering
University of Padua
35131 Padua, Italy
matteo.camporese@unipd.it

ARTICLE IN PRESS

ARTICLE IN PRESS

Keywords: protected agriculture; water cycle; integrated surface–subsurface hydrological modelling; CATHY; greenhouse climate modelling

ARTICLE IN PRESS

ARTICLE IN PRESS

Abstract

Greenhouse agriculture is increasingly vital for food security. Yet, its catchment-scale hydrological effects remain poorly understood. We develop an integrated framework combining greenhouse climate modelling and remote sensing of land cover with the physically based CATchment HYdrology (CATHY) surface–subsurface hydrological model. We apply it to the *Piana del Sele* district in southern Italy to assess trade-offs under land use and climate change scenarios. Our simulations show that, compared to open fields, greenhouses theoretically reduce evapotranspiration; however, their effects on irrigation requirements depend strongly on the timing of crop cycles relative to rainfall. Moreover, greenhouses increase streamflow and reduce groundwater storage. Climate change intensifies summer irrigation demand, although halting greenhouse cultivation in summer mitigates this pressure. These results demonstrate how greenhouse expansion reshapes regional water balances and highlight the need for integrated modelling to inform water management and provide a transferable basis for policies balancing food production and water security.

ARTICLE IN PRESS

ARTICLE IN PRESS

Introduction

Agriculture is the economic sector that uses the largest share of freshwater, achieving values up to 90%, globally, with some countries in North Africa and Middle East withdrawing ten times more water than what is available to them[1]. Agriculture water use often drives the depletion of both surface water and groundwater resources, exposing connected ecosystems to detrimental impacts in dry periods[2,3]. Freshwater resources depletion will likely be exacerbated by the growing demand for food to meet the needs of an increasing human population as well as due to the projected increase of incoming solar longwave irradiance[4], which will increase crop transpiration[5] as long as soil water is available[6]. Climate change is also driving more severe and frequent hazardous meteorological phenomena, alternating longer-lasting droughts with shorter and more intense rainfalls, as well as increased seasonal variability in precipitation[7]. These weather-related factors could strongly increase crop losses.

Greenhouse cultivation is a technological solution that allows farmers to decouple food security from meteorological conditions. In its simplest form, greenhouses are built by covering soil-grown crops with plastic films supported by a metal frame, without an active climatic control and with a sprinkler irrigation system (here referred to as plastic greenhouses)[8]. The expected effects of protected agriculture on hydrological processes at the catchment scale are represented in Fig. 1.

It is common knowledge that the rain falling on traditional open-field crops is partitioned between interception on crop leaves, runoff, infiltration through the soil, and ponding on the ground. On the other hand, the rain falling on a greenhouse cover is either stored in tanks or

ARTICLE IN PRESS

ARTICLE IN PRESS

retention ponds for different purposes, such as irrigation[9,10,11], or it is conveyed to the drainage system, in this case leading to faster flow generation and, therefore, higher discharge peaks. Greenhouse conditions ensure reduced solar radiation and wind speed, increased air temperature, and build-up of air moisture[12]. Climate data collected inside greenhouse facilities corroborate that these climatic conditions result in decreased evapotranspiration (ET)[13]. This evidence has prompted the development of empirical equations to estimate ET inside greenhouses, such as a modified version of the widely known Penman-Monteith equation[14], proposed by Fernández et al.[15]. Thanks to the possibility of relying on less water, intensive horticulture production under plastic greenhouses flourishes where sunlight is abundant, even in rural, semi-arid and water-scarce areas[12,16]. Moreover, innovative materials can further reduce irrigation water use in greenhouses by absorbing air moisture at high relative humidity during the night and releasing water for irrigation during the day using natural sunlight[17]. Greenhouse cultivation is expanding along the Mediterranean Sea coasts, such as the Almería region in Spain, the Anamur district in Turkey, the surroundings of Marina di Acate in Italy, and the Ierapetra district in Greece[18]. In 2019, a total of 13,000 km² of greenhouse infrastructure was identified worldwide[19]. Most of this infrastructure is concentrated in large facilities, with 61% of greenhouse districts having an area greater than 15 km². While these facilities are primarily concentrated in China (60%), they were also observed to be increasing in the Global South, particularly in Mexico and Morocco[20]. The *Piana del Sele* (Fig. 2) in the Campania region, southern Italy, exemplifies this phenomenon, where the proliferation of plastic greenhouses has transformed the region into a strategic hub for food commodities exported throughout Europe. This, however, has led to severely increased flood risk; consequently, the Campania region has

ARTICLE IN PRESS

ARTICLE IN PRESS

legislated the building of Low Impact Development (LID) solutions next to new greenhouses as a measure to maintain the hydraulic invariance of the farm and to therefore reduce the risk of inundation of downstream agricultural lands (Regional Law 33/2012).

The consequences of land use change and climate change on the catchment hydrological response can be assessed by means of integrated surface–subsurface hydrological models (ISSHMs)[21,22,23,24]. This makes coupling greenhouse environment models with ISSHMs an appropriate choice for studying the short- and long-term dynamics of surface water and groundwater in agricultural catchments affected by the expansion of plastic greenhouse districts. Here, we combine a greenhouse environment model to simulate the indoor environment given outdoor meteorological variables[25] with the CATchment HYdrology (CATHY) model[26] to simulate coupled surface–subsurface water flow and with remote sensing satellite data to provide land cover information[18,27]. The developed workflow is schematized in Fig. 3. This modelling framework is applied to a ~10 km^2 agricultural catchment covered mostly by multi-tunnel plastic (polyethylene) greenhouses in the *Piana del Sele*. This area is one of the largest vegetable production districts in Italy and the main production area for some cut leafy vegetables, such as arugula, in Europe. Therefore, it is representative of the response of similar districts, especially in the Mediterranean area. Our study examines the impact of plastic greenhouses on various hydrological factors in agricultural catchments, including evapotranspiration, stream discharge, saturated groundwater storage, and irrigation requirements. We conduct simulations at two distinct time scales: a short-term 14-month period to highlight the immediate effects on streamflow response of intense rainfall events, and a long-term 65-year period to analyse how

ARTICLE IN PRESS

ARTICLE IN PRESS

greenhouse districts respond to projected climate changes. To better understand the greenhouse horticulture effects, we compare three land use scenarios for the study area at both time scales: no greenhouses, current land cover (partial greenhouse coverage), and complete greenhouse coverage (Fig. 3). This approach allows us to comprehensively assess the environmental consequences of greenhouse expansion in the region. To the best of our knowledge, this is the first study coupling a mechanistic plastic greenhouse climate model with a physics-based ISSHM to quantify water balance trade-offs at the catchment scale under both land use and climate change scenarios.

ARTICLE IN PRESS

Results

Potential evapotranspiration for various land uses

We first evaluate how various land uses affect evapotranspiration for the short-term study period (June 2023–January 2025). Potential crop evapotranspiration (ET_C) has been computed as shown in Fig. 3 for the separate land uses applied in the study area, i.e., i) greenhouse cultivation (ET_c^G); ii) open-field winter crops ($ET_c^{OF\text{-}winter}$); iii) open-field summer crops ($ET_c^{OF\text{-}summer}$); and for iv) the actual mix of open-field winter and summer crops (ET_c^{OF}), assessed through an area-weighted monthly varying crop coefficient derived from Sentinel-2 satellite imagery (Supplementary Fig. 1b) and excluding greenhouses.

Cumulative ET_0 is 1,400 mm for greenhouses and 1,800 mm for the mixed open fields (Supplementary Fig. 1a), confirming that reference evapotranspiration is lower under greenhouse conditions. In greenhouses, ET_c is lower than ET_0 and amounts to 900 mm due to the absence of crops during the summer (K_c = 0 in June and July), when most farmers apply

ARTICLE IN PRESS

solarization—a practice that sterilizes the soil by exploiting high temperatures inside the greenhouses (Supplementary Fig. 1c). The typically dry summer in the *Piana del Sele* makes solarization advantageous, as irrigation needs would otherwise be excessive. This practice also aligns greenhouse crop cycles with periods of higher rainfall, potentially allowing for rainwater storage and reuse (not currently exploited).

The remote sensing-based NDVI (Normalized Difference Vegetation Index) time-series analysis[28] indicates a predominance of winter crops over summer crops as the open-field condition in the study area. The analysis identified vegetated areas and prescribed $K_C = 1$ when NDVI > 0.4. Using the calculated area-weighted K_c for open-field crops (Supplementary Fig. 1b) to reflect both the proportions of winter and summer crops by month, the average ET_c is 760 mm (Supplementary ET_c^{OF} in Fig. 1c). A typical winter crop (assuming $K_C = 1$ from November to April and $K_C = 0$ otherwise) requires only 405 mm over its 6-month phenological cycle, closely matching the rainfall season. In contrast, a summer crop (assuming $K_C = 1$ from May to October and $K_C = 0$ otherwise) requires up to 1,390 mm over 6 months, with peak water demand during the driest months, making irrigation essential to sustain yields. Overall, the predominance of winter crops in open fields results in ET_c^{OF} being similar to ET_C^{G}.

Effects of greenhouses on streamflow in the short and long terms

In the short term, the replacement of greenhouses with open-field winter crops showed a substantial decrease in the simulated streamflow intensity as compared to the reference land use (Fig. 4a). In contrast, in the case of a continuing expansion of greenhouses in the place of open fields, the model output results in higher streamflow peaks (Fig. 4a) and runoff volume.

ARTICLE IN PRESS

ARTICLE IN PRESS

Assuming a threshold of 10 $m^3 s^{-1}$, the simulations show that it was exceeded by the peak streamflow in the greenhouse scenario in 10 events (we excluded the extreme peak of over 40 $m^3 s^{-1}$ because the other scenarios did not show any response to the same rainfall event). In these 10 events, the streamflow in the greenhouse-only scenario is on average 80% higher than the streamflow in the reference scenario, while the streamflow in the open field-only scenario is on average 30% less than the streamflow in the reference scenario.

The implications of removing greenhouses, maintaining the current reference scenario, and increasing the presence of plastic greenhouses in the context of long-term climate change are broadly consistent with the results obtained in the short-term simulations. Expansion of greenhouses increases land surface imperviousness, and because rain cannot infiltrate into the soil, this scenario generates the largest cumulative overland flow volume, with an increase of 15.8% with respect to the reference scenario (Fig. 4b) over 65 years. In contrast, antecedent land use conditions without greenhouses generates the smallest cumulative overland flow volume, with a reduction of 5.6% compared to the reference scenario (Fig. 4b).

ARTICLE IN PRESS

Impacts of greenhouses on groundwater storage depth in the short and long terms

Groundwater storage and its dynamics are important indicators of groundwater availability for drinking and irrigation purposes[29]. Under the short-term simulation and in the current land use scenario (the reference), the CATHY model simulates a seasonal variability in the groundwater storage depth, with a minimum depth of about 0.5 m in summer and an average depth of about 0.7 m over the year (Fig. 5a). Summer is typically very dry and is characterized by a substantial loss of groundwater storage depth. The abundant rainfalls in autumn and winter are essential to

ARTICLE IN PRESS

recover the groundwater storage depth after the summer period. The hypothetical open field-only scenario, simulating the presence of winter crops in the place of greenhouses and with the mix of summer and winter crops in the remaining agricultural areas, reveals not only that the whole soil profile frequently saturates in the rainy seasons (Fig. 5a), but also that only 10 cm of groundwater storage depth are lost in summer. This is due to winter crops i) not using any water from May to November, whereas greenhouses only stop operating in June and July (Fig. 3 and 4c), and ii) allowing infiltration and groundwater recharge once rain starts again in September, contrary to the greenhouses. The last scenario, representing the expansion of greenhouse horticulture over the whole available agricultural area, exhibits a much less variable saturated storage, due to the decoupling of most of the catchment area from natural atmospheric fluxes (Fig. 5a). However, the average groundwater storage remains 5 cm less than in the open field-only scenario. It is important to note that these values represent conservative estimates, since the simulation scenarios do not consider the use of groundwater for irrigation.

Climate change ultimately decreases the groundwater storage depth across the three land use scenarios (Fig. 5b), implying less availability of groundwater for drinking water supply, irrigation, and groundwater-dependent ecosystems. The reference land use shows a groundwater storage depth ranging between the lowest values reached in the greenhouse scenario and the highest values achieved in the open field-only scenario (Fig. 5b). The linear trend of groundwater storage depths for the three land use scenarios is always decreasing. The open field-only scenario is the one with the smallest decrease (0.64 mm y^{-1}), while the negative trend of the groundwater storage depths for the reference and greenhouse scenarios is the same (1.14 mm y^{-1} in both scenarios) (Fig. 5b). This result highlights a notable nonlinearity in the groundwater storage depth

ARTICLE IN PRESS

ARTICLE IN PRESS

considering that an average greenhouse cover of about 40% (Table 1) in the reference scenario suffices to drive a storage loss rate equal to the greenhouse-only scenario, in which 30% of agricultural fields in the reference land use (Table 1) are converted to greenhouse horticulture. However, once again, the simulations do not consider the use of groundwater for irrigation, which is expected to be larger for the greenhouse-only scenario.

Effects of greenhouses on irrigation water demand and supply in the short and long terms

The irrigation water demand was assumed to match crop evapotranspiration (ET_C), in line with local practices. In the reference simulation scenario, the irrigation demand is only slightly higher than the irrigation demand for the greenhouse-only scenario (Fig. 6a). This is because in the latter scenario greenhouses replace mostly winter crops, which are characterized by a shorter growing season and low crop evapotranspiration, comparable with the reduced ET_C we can expect under greenhouses. However, the supplied irrigation in the reference scenario, calculated using the CATHY model which accounts for available soil moisture, is 55% of the demand (Fig. 6b) because winter crops receive rainfall, which contributes to meet the crop water demand . In contrast, in the greenhouse-only scenario the supplied irrigation must match the demand, resulting in a higher irrigation water consumption. Finally, the open field-only scenario, where all the greenhouses are replaced by winter crops, exhibits reduced irrigation demand (approximately 40% less than the reference value, as shown in Fig. 6a) and an extremely low supply (1.7% of the demand; note the log scale of the y-axis in Fig. 6b), thanks to rainfall which is mostly synchronised with demand.

ARTICLE IN PRESS

ARTICLE IN PRESS

In the the long-term climate change simulations, rainfall decreases in all seasons except in winter, for which a clear trend was not observed (Fig. 7). For open-field crops in the reference scenario, the lack of rainfall in relation with the timing of the irrigation water demand calls for a six-fold increase in supplied irrigation volumes in autumn (from 0.01 million m^3 per season on average for the period 2017-2026 to 0.06 million m^3 per season for the period 2057-2070) and a five-fold increase in summer (from 0.02 million m^3 per season on average for the period 2017-2026 to 0.1 million m^3 per season for the period 2057-2070). The open field-only scenario (winter crops in the place of greenhouses) substantially reduces the irrigation water supply both in autumn (average of 0.01 million m^3 per season for the period 2057-2070) and in summer (average of 0.015 million m^3 per season for the period 2057-2070). This result can be explained by the higher groundwater storage in the open field-only scenario, which can be used by summer crops to meet their water demand. In spring and winter, there are no clear trends in supplied irrigation volumes despite the substantial decrease in rainfall in both the reference and open field-only scenarios. Nor are there substantial differences in irrigation volumes between the two scenarios under examination. A plausible reason for this is the general minimal ET_C in combination with adequate soil moisture replenished by infiltrating rainwater.

Greenhouses cause a decoupling between the crop water demand and atmospheric conditions; therefore, expanding the area of greenhouses from the reference scenario to the greenhouse-only scenario results in a proportional increase in the irrigation water supply, which in this case must match the demand, in all seasons, shown as a shift toward higher irrigation volumes between scenarios in Fig. 7b. Interestingly, an increase in irrigation volume is evident in the

ARTICLE IN PRESS

ARTICLE IN PRESS

greenhouse scenario in the spring. This result can be attributed to the projected increasing temperatures in spring, driving rising ET_c and the consequent water demand.

Discussions

Previous studies on the large-scale effects of plastic greenhouses focused mainly on meteorological aspects. For instance, Campra & Millstein[30] found that greenhouses in Almeria (Spain) could lower air temperatures by 0.5 °C . Our study provides evidence on how plastic greenhouse expansion alters catchment-scale water dynamics, revealing trade-offs between local water savings and regional hydrological sustainability. We found that greenhouse systems reduce evapotranspiration compared to open-field farming. While this would theoretically translate to lower irrigation demand, in practice it depends on the relative timing of crop cycles and rainfall. Our integrated modelling shows that in Mediterranean agricultural districts, rain-fed winter crops require the lowest volume of additional irrigation water thanks to both low evapotranspiration and the contribution of rainfall to replenish soil moisture. Conversely, summer crops would require the highest volume of irrigation water because of high evapotranspiration and asynchronicity with the rainfall season. Greenhouse horticulture is practised when rainwater is potentially available, but this is not currently exploited. Thus, the source of irrigation water becomes an important consideration. In the study area, open-field crops are preferably irrigated with surface water diverted from the Sele River and provided by the local water authority through irrigation canals. In contrast, greenhouse farmers use private deep groundwater wells for assuring chemical and microbiological quality, which allows them to produce compliant ready-to-eat vegetables for European markets. This need for exceptionally

ARTICLE IN PRESS

ARTICLE IN PRESS

clean water may result in limitations to the harvesting of rainwater from greenhouse roofs or other reuse strategies. Greenhouse districts also come at the cost of higher surface runoff and decreased groundwater storage. The hydrological balance is therefore shifted: while farmers may benefit from reduced water needs compared to open-field summer crops, the catchment as a whole faces increased risks of soil moisture depletion, aquifer decline, and greater flood peaks. These results highlight that efficiency at the field scale does not automatically translate into sustainability at the landscape scale.

Climate change further amplifies these tensions. Simulations indicate that hotter and drier summers substantially increase irrigation requirements, particularly under greenhouse-only scenarios. A simple adaptation measure—halting greenhouse cultivation during peak summer months—proved effective in mitigating water stress. Aligning greenhouse production cycles with rainfall harvesting could thus play a decisive role in maintaining long-term water security, provided water quality meets the expected standards. This study relied on a single climate change scenario; thus our results should not be interpreted as definitive projections for decision-making, but rather as an investigation, under robust tendencies, into which types of water management strategies and cropping practices may be most effective in guiding future adaptation actions. Indeed, the adopted scenario is consistent with one of the most robust signals of climate change, in particular over the Mediterranean region, where warming is already about 20% higher than the global mean and is expected to further intensify[31]. In addition, increasing water scarcity and reduced rainfall are recognised among the main climate risks for Europe[32]. More specifically, in the Italian National Adaptation Plan for Climate Change[33], this pattern is reported for central and southern Italy[33]. Within this framework, our simulations

ARTICLE IN PRESS

ARTICLE IN PRESS

indicate that lower rainfall and higher summer temperatures will disproportionately increase irrigation demand in open-field conditions, whereas greenhouse practices will curb the increase in water requirements.

The increased flood risk in plastic greenhouse districts and in cities share the same root cause, which is attributable to a growing imperviousness of catchments[34]. Therefore, just as cities are turning to Low Impact Development practices to mitigate the risk of urban flooding, greenhouse districts should follow suit. However, structural adaptation measures, such as LID practices, may not adequately address groundwater decline if they are designed solely to preserve hydraulic invariance. We argue that such measures should be reframed not only as tools for runoff control, but also as opportunities for managed aquifer recharge and water reuse. This dual benefit would support both farmers' resilience and downstream water users.

ARTICLE IN PRESS

Conclusions

Our analysis has focused on a single district in southern Italy; nonetheless, the results are widely transferable. Greenhouse agriculture is rapidly expanding across the Mediterranean, Latin America, and Asia, often in regions already facing water scarcity. The mechanisms we describe—reduced ET, altered groundwater storage, and increased runoff—are intrinsic to greenhouse cultivation and thus relevant well beyond our case study. Our modelling framework, which bridges hydrology, agriculture, and remote sensing, provides a replicable approach for assessing these impacts in other regions. Overall, our results underscore the need for integrated policy and management strategies that go beyond farm-scale efficiency. Effective governance of

ARTICLE IN PRESS

greenhouse agriculture must reconcile food production with water security, anticipating the dual pressures of land-use intensification and climate change.

Methods

Study area

The study area is a medium-sized agricultural catchment (9.9 km^2) in the *Piana del Sele* (Italy) with a land surface coverage by plastic greenhouses of about 40% (and increasing). The region is characterized by a Mediterranean climate. According to ERA5 data for the climatology period from 1991 to 2020[35], yearly rainfall is 1,134 mm and is concentrated in autumn and winter, with temperatures ranging between an average minimum of 6 °C in January and an average maximum of 27.8 °C in August. The catchment elevation ranges between 5 m and 20 m, with a mean gentle slope of 0.02% toward the sea, as calculated from the digital elevation model (DEM) TINITALY. This DEM product represents the surface of Italy without vegetation and development, available at 10 m cell resolution[36].

The area used to be a swamp until about fifty years ago, when the land was reclaimed. The *Piana del Sele* consists of Quaternary geologic deposits, with alternating layers of sand and gravel and with high porosity and permeability, separated by impermeable layers of silt and clay. The first impermeable layer was found at 5 m depth and the water table was about 1.5 m deep (Source: geological survey carried out in 2010 for the renovation of the drainage channels). Upstream, the *Piana del Sele* is surrounded by calcareous-dolomitic reliefs, with karstic aquifers, through which water can flow and reach a multitude of irregularly stratified aquifers at different depths.

ARTICLE IN PRESS

ARTICLE IN PRESS

Land use

Land cover at the parcel level was manually digitized using Google satellite images (May 2023), since detailed and up-to-date cadastral data were not available. The resulting vector file distinguished six land cover classes (Table 1). A representative root depth was assigned to each class (Table 1), assuming a linear decrease of root density with depth.

To capture the spatial and temporal variability of land cover during the modelling period, we used Sentinel-2 L2A satellite imagery. The Open Agriculture and Protected Agriculture Classifier (OPAC[18]) was applied to monthly aggregated Sentinel-2 data in the Google Earth Engine platform[26]. This classification identified three categories: protected agriculture (plastic greenhouses), vegetated (land cover with vegetation), and bare soil (no vegetation). For each grid cell of the computational domain, the NDVI[28] was also extracted.

Crop coefficients were then prescribed according to land cover type. Greenhouses (class ID 1 in Table 1) were assigned a coefficient of 1 from August to May and 0 for June and July, reflecting the local practice of halting cultivation in summer due to high internal temperatures and applying soil solarization. Open agriculture classes (IDs 3 and 4) were assigned a coefficient of 1 for NDVI > 0.4, and 0 otherwise. All remaining classes (IDs 2, 5, and 6) were considered non-vegetated.

Hydro-meteorological data

Weather data at 10-minute resolution were obtained from the nearest gauging station at Battipaglia (hereafter BA), operated by the Agriculture Office of the Campania Region (AOCR). The BA station is located at 40°35’5.6602” N, 14°58’53.26” E, at an elevation of 46 m a.s.l., and

ARTICLE IN PRESS

ARTICLE IN PRESS

lies about 6.2 km from the catchment outlet. The dataset included rainfall (P) and all variables required to calculate reference evapotranspiration (ET_0) for both open-field and greenhouse conditions: air temperature (2 m above ground), relative humidity, wind speed (2 m), and global solar radiation.

Outdoor ET_0 was calculated following the FAO method for hourly data[14], as implemented by la Cecilia et al.[37]. Indoor hourly ET_0 was estimated with a greenhouse climate model[25,38], previously evaluated for the study area. This model simulates indoor climate conditions from outdoor weather and applies a modified Penman–Monteith equation[15] to account for greenhouse environments. Possible negative values during night or early morning were set to 0 mm h^{-1}.

Missing data were filled using measurements from a nearby station at Eboli (40°33'13.3" N, 14°58'49.8" E), also maintained by AOCR and located 3.5 km away from the catchment and about 7.5 km from the outlet. Any remaining gaps were filled with the corresponding hourly value from the previous day, except for rainfall, which was set to 0 mm h^{-1}. Weather data were assumed to be spatially homogeneous across the catchment.

At the outlet, a high-precision Keller Series 36XiW-CTD probe (Switzerland) was used to measure water depth (via pressure), electrical conductivity, and temperature. The outlet cross-section consists of a 2.5 m wide, 0.5 m high rectangular channel, transitioning into a trapezoidal section with a minimum width of 7.5 m and a maximum width of 11.0 m, with a height of 2.4 m. The rating curve was numerically derived using the Engelund method[39] in combination with the Gauckler–Strickler formula to compute discharge Q (m^3 s^{-1}) for water depths between 0 and 2.4 m.

ARTICLE IN PRESS

ARTICLE IN PRESS

Evapotranspiration calculation for the comparison between mixed open-field agriculture, greenhouse horticulture, and separate summer and winter crops

For the reference land use with a mix of summer and winter crops in open fields, we calculated an area-weighted monthly crop coefficient (K_c) using Sentinel-2 imagery. In practice, the K_c for open-field agriculture changed spatially and monthly depending on the growth stages of summer and winter crops (Supplementary Fig. 1b). Using satellite data, we prescribed $K_c = 1$ to those cells falling in the aggregated land cover "open-field agriculture" (Table 1) with NDVI > 0.4, and $K_c = 0$ otherwise. Thus, the number of cells with $K_c = 1$ for open-field conditions was divided by the total number of open-field cells per month in the short-term period. This area-weighted monthly K_c was multiplied by the corresponding hourly ET_0 values to obtain the area-weighted evapotranspiration for the mixed land-use reference scenario.

For crop cycles, we prescribed the following seasonal K_c values:

- Winter crop: $K_c = 1$ from November to April; $K_c = 0$ otherwise.
- Greenhouse crop: $K_c = 1$ throughout the year, except June–July, when $K_c = 0$ (to account for halted cultivation during soil solarization).
- Summer crop: $K_c = 1$ from May to October; $K_c = 0$ otherwise.

CATchment HYdrology model (CATHY)

CATHY is a physics-based integrated surface–subsurface hydrological model that explicitly represents the interactions between surface water, groundwater, and vegetation. Its subsurface module solves the three-dimensional Richards equation for variably saturated porous media,

ARTICLE IN PRESS

ARTICLE IN PRESS

while the surface module solves the diffusion-wave approximation of the shallow water equations[26].

Given the agricultural setting of the catchment, we assumed that actual evapotranspiration (ET) is equal to root water uptake. Root water uptake in CATHY is computed using the Feddes approach[40], which applies a water stress function α(ψ) dependent on the pressure head ψ. Accordingly, actual evapotranspiration is calculated as $ET_C \times \propto(\psi)$, where the stress function is defined as:

$$\propto(\psi) = \begin{cases} 0 \text{ when } \psi < \psi_{wp} \\ \dfrac{\psi - \psi_{wp}}{\psi_d - \psi_{wp}} \text{ when } \psi_{wp} < \psi < \psi_d \\ 1 \text{ when } \psi_d < \psi < \psi_{an} \\ 1 - \dfrac{\psi - \psi_{an}}{\psi_s - \psi_{an}} \text{ when } \psi_{an} < \psi < \psi_s \\ 0 \text{ when } \psi > \psi_s \end{cases}$$

Here, ψ_{wp} is the pressure head at the wilting point, ψ_d is the pressure head threshold at which vegetation begins to experience stress, ψ_{an} is the anaerobiosis limit beyond which excess soil water impairs plant function, and ψ_s is the pressure head at saturation. The pressure head parameters used in the Feddes model are the same for both greenhouse and open-field conditions and are listed in Table 1.

For all simulations, we prescribed a fixed Gauckler–Strickler coefficient of 40 $m^{1/3}\ s^{-1}$ for stream channels, reflecting concrete channels partially covered by vegetation. Roughness coefficients

ARTICLE IN PRESS

were also set to 40 $m^{1/3}$ s^{-1} for cells with greenhouses and 1 $m^{1/3}$ s^{-1} for open-field agriculture, based on manual calibration.

CATHY quantifies storage changes and fluxes across fixed and moving boundaries (i.e., the water table) of the subsurface saturated zone based on the numerical resolution of the weak formulation of the Richards equation[41]. The groundwater storage depth is hereby defined as the water storage in the subsurface saturated zone[41]. The computed depth is based on water volume integration over the time-variable saturated zone, depending on seasonal aquifer fluctuations and soil stratigraphy and hydraulic properties. The groundwater storage depth is here utilized as a metric to assess the effects of the greenhouses on both short-term and long-term aquifer water availability at the catchment scale.

ARTICLE IN PRESS

Model set-up

We down-sampled the DEM to an 80 m resolution, which provided a good balance between retaining sufficient detail for simulating the catchment with hourly boundary conditions and maintaining feasible computational demands. This resolution allowed the model to run efficiently on personal computers with up to 16 GB RAM.

Because DEM values were not always monotonically decreasing along the main channel, manual adjustments were required to define a consistent drainage network from upstream to downstream. Specifically, the minimum DEM value was set at the outlet cell, and the values of DEM cells intersected by the manually digitized channel were modified to ensure a consistent gradient from downstream to upstream. Notably, the land reclamation authority applied similar slope corrections during channel restoration to prevent ponding.

ARTICLE IN PRESS

The adjusted DEM was used to generate the computational mesh of the catchment. The final numerical grid included 13 vertical layers and comprised 23,688 nodes and 119,808 tetrahedral elements.

Soil type and numerical representation

Based on stratigraphic information, we represented a total soil thickness of 2 m, with an impermeable layer prescribed as the bottom boundary condition. The soil column was discretized into thirteen numerical layers parallel to the ground surface, with thickness gradually increasing with depth. The discretization intervals were: 5 cm from the surface to 10 cm (2 layers), 10 cm between 10–40 cm (3 layers), 20 cm from 40 cm to the bottom (8 layers).

According to soil management practices and a previous geological survey indicating low hydraulic conductivity, we assumed a loamy soil at the surface and silty clay at depth. This soil classification is broadly consistent with data from the SOILGRIDS database[42]. Hydraulic parameter values for these two soil types were taken from Carsel & Parrish[43] (Table 2) and interpolated exponentially across the discretized soil depths.

To account for the influence of plastic greenhouses on rainfall partitioning between runoff and infiltration, we reduced the vertical hydraulic conductivity of the topsoil layer to 1×10^{-10} m s^{-1}, consistent with values for plastic membranes. Soil water retention and unsaturated hydraulic conductivity were calculated using the van Genuchten model[44], with parameter values listed in Table 2.

Atmospheric forcing and boundary conditions

ARTICLE IN PRESS

ARTICLE IN PRESS

Irrigation demand was set equal to the estimated daily crop evapotranspiration (ET_c), separately calculated for greenhouse (ET_c^G) and open-field (ET_c^{OF}) conditions.

In the open fields, the actually supplied irrigation was calculated by the CATHY model based on current water saturation (S_w) conditions and may be lower than the irrigation demand, because of rainfall contributing to increase the soil water content and partially meeting the crop evapotranspiration demand. This process was simulated through a new module in CATHY[45] that regulates the irrigation rate supplied to each surface node. The routine inhibits irrigation whenever S_w exceeds a user-defined threshold (set at 0.35 for this study). Irrigation for open-field crops (land cover classes 3 and 4 in Table 1) was applied as an atmospheric flux boundary condition in a single daily event scheduled from 9:00 to 10:00.

For greenhouses (land cover class 1 in Table 1), supplied irrigation was assumed equal to the irrigation demand as crops cannot be rain-fed. In this case, irrigation fluxes were applied as source terms in the third soil node layer from the surface—below the low-conductivity layer representing the plastic cover. This was scheduled as a single event from 9:00 to 12:00.

Net precipitation (rainfall minus ET_c) was prescribed as atmospheric forcing for open-field crops (with $ET_c = ET_c^{OF}$) and for greenhouses (with $ET_c = ET_c^G$), while rainfall alone was applied to other land covers. At the bottom of the domain, no-flux boundary conditions were imposed to represent the underlying low-conductivity layer.

Reference scenario

The short-term simulations were initialized with a warm-up period of approximately 180 days (1 June–30 November 2023), using hourly weather data avalable previous to the collection of water

ARTICLE IN PRESS

ARTICLE IN PRESS

level measurements. The initial condition was set as a spatially uniform water table at 2.0 m depth, consistent with antecedent geological surveys.

A preliminary sensitivity analysis, in which the initial water table depth was varied from fully saturated to unsaturated conditions, confirmed that the warm-up period was sufficient to minimize the influence of initial conditions.

The short-term simulation period, used also to assess the model performance, was 1 December 2023 to 31 January 2025. This interval matched the availability of both high-frequency water level records at the outlet (5-minute resolution) and hourly outdoor weather data.

CATHY model calibration

The CATHY model was calibrated against observed discharge at the outlet by manually tuning the Gauckler-Strickler coefficients of hillslope and channel cells, to ensure that the model could realistically capture the catchment's runoff response to rainfall events. The hydrometeorological forcings input to the CATHY model were the measured rainfall, uniform over the whole catchment, as well as the calculated potential crop evapotranspiration for open-field and greenhouse crops and the corresponding irrigation rates, variable in space depending on land use and the crop phenological stage.

The model performance was evaluated through the Kling–Gupta Efficiency (KGE) index[46]. Considering the relatively short monitoring period spanning 14 months and the clear climatic seasonality of the study area, the entire streamflow time series was necessary to calibrate the model, and no split validation was possible. The calibrated CATHY model was able to reproduce the magnitude and duration of the streamflow during rainfall events (Fig. 8), achieving a KGE

ARTICLE IN PRESS

ARTICLE IN PRESS

index of 0.66 after correcting for the baseflow. This correction was needed as the baseflow in the main collector is maintained by three external sources. Two sources are continuous and come from an artesian well and an upstream field channel. The third source is seasonal, a dual drainage/irrigation canal that enters the catchment through a gate in the summer period. While it would have been possible to introduce directly into the model a dynamic input time series for the inlet streamflow, it was deemed that this implementation would not bring additional hydrological understanding. Therefore, we simply corrected the simulated streamflow to account for the measured baseflow. For the baseflow correction, we identified eight time intervals during which changes in measured streamflow could not be attributed to meteorological drivers. For each time interval, we calculated a piece-wise linear trend between the initial and final streamflow measured. Finally, the trends were added to the simulated streamflow. The time intervals and initial and final streamflow values are reported in Supplementary Table 1.

One of the main uncertainties affecting the simulations is likely related to the spatial variability of rainfall measurements. In fact, the comparison of two weather stations measuring at hourly intervals, located upstream and downstream of the study area, 10 km away from each other, revealed different rain patterns and intensities. This has implications on the simulated streamflow, most substantially between days 270 and 280 after 1 December 2023 when the measured discharge reached very high values, ostensibly in response to relatively low rainfall in terms of intensity and duration.

Land use scenarios

ARTICLE IN PRESS

ARTICLE IN PRESS

In addition to the calibrated hydrological model, we simulated two contrasting land use change scenarios and evaluated their impacts:

1. **Open field-only scenario**

The first scenario dated back to about 1980 when greenhouses were absent (Fig. 2b). Based on the traditional predominant cultivation of winter crops, confirmed by vegetation indices from satellite imagery, greenhouses were replaced with winter crops in open-field conditions. Correspondingly:

- the top soil hydraulic properties were adjusted to represent open-field conditions;
- irrigation was applied to winter crops as an atmospheric boundary condition;
- the Gauckler–Strickler roughness coefficient for greenhouses (40 $m^{1/3}$ s^{-1}) was replaced with the value for open fields (1 $m^{1/3}$ s^{-1}).

2. **Greenhouse-only scenario**

In this scenario, all open-field crops were replaced with greenhouses to explore the potential effects of continued greenhouse expansion, as suggested by historical satellite images (Fig. 2b to e). Accordingly:

- the top soil hydraulic properties were updated to reflect greenhouse conditions;
- irrigation was supplied to greenhouse leafy vegetables as a source term;
- the Gauckler–Strickler coefficient for open fields (1 $m^{1/3}$ s^{-1}) was replaced with the greenhouse value (40 $m^{1/3}$ s^{-1}).

Long-term climate change scenario

ARTICLE IN PRESS

ARTICLE IN PRESS

The three land use scenarios hypothesized for the short-term simulations with corresponding parametrizations – of soil, land use, crop coefficients, Gauckler-Strickler coefficients - relative to the year 2024 were replicated in the long-term climate change scenario. Rainfall and the meteorological variables for calculating ET and the corresponding irrigation for open-field and greenhouse conditions with an hourly time step and spanning from 2006 to 2070 were derived from a convection-permitting regional climate simulation at 2.2 km resolution[47]. This dataset was obtained by dynamically downscaling the CMCC-CM global climate model under the IPCC RCP8.5 scenario using the COSMO CLM model in a specific configuration developed for Italy. The configuration, resolving convective processes explicitly, provides a physically consistent representation of precipitation extremes and local-scale atmospheric dynamics, which are particularly relevant for the innovative application presented in this study as well as those applications reported by Coppola et al.[48] The dataset provided rainfall (P), air temperature (2 m above ground), relative humidity, wind speed (2 m), and global solar radiation. Outdoor ET_0 was calculated following the FAO method for hourly data[14], as implemented by la Cecilia et al.[37] Indoor hourly ET_0 was estimated with a greenhouse climate model[25]. Negative values during night or early morning were set to 0 mm h^{-1}. Weather data were assumed to be spatially homogeneous across the catchment.

ARTICLE IN PRESS

Declaration of competing interest

The authors declare no competing interests.

Correspondence should be addressed to Daniele la Cecilia or Matteo Camporese.

ARTICLE IN PRESS

Data Availability

All input and output data together with models are available through the University of Padova research data archive (https://researchdata.cab.unipd.it/) to ensure that these data are FAIR: Findable, Accessible, Interoperable and Reproducible. Weather data were asked by means of an agreement to the Agriculture Office of the Campania region. Water level data were measured using our own sensor installed for the purpose of the project. Satellite data were obtained using the Google Earth Engine Platform. Climate change data are available at https://dds.cmcc.it/#/dataset/climate-projections-rcp85-downscaled-over-italy/rcp85 thank to the "HIGHLANDER" project carried out by CINECA, CLM Assembly and CMCC.

Code Availability statement

The greenhouse climate model is written in R and available at 10.25430/researchdata.cab.unipd.it.00001493. The CATHY model used in this study is freely available at 10.25430/researchdata.cab.unipd.it.00001710

References

1. FAO, (2022). AQUASTAT Core Database. Food and Agriculture Organization of the United Nations. Database accessed on 2024/03/23.
2. Green, A.J. et al. Groundwater Abstraction has Caused Extensive Ecological Damage to the Doñana World Heritage Site, Spain. Wetlands 44, 1-13 (2024).

ARTICLE IN PRESS

ARTICLE IN PRESS

3. Jägermeyr, J. et al. Reconciling irrigated food production with environmental flows for Sustainable Development Goals implementation. Nat Commun 8, 15900 (2017).
4. Roderick, M.L. et al. A general framework for understanding the response of the water cycle to global warming over land and ocean. Hydrol. Earth Syst. Sci. 18, 1575–1589 (2014).
5. Mastrotheodoros, T. et al. More green and less blue water in the Alps during warmer summers. Nat. Clim. Change 10, 155–161 (2020).
6. Dong, J. et al. Can surface soil moisture information identify evapotranspiration regime transitions? Geophys. Res. Lett. 49, e2021GL097697 (2022)
7. Wade, C.M. et al. Opportunities and spatial hotspots for irrigation expansion in Guatemala to support development goals in the food-energy-water nexus. Agric. Water Manag. 267, 107608 (2022).
8. Pérez Parra, J. et al. Natural ventilation of parral greenhouses. Biosyst. Eng 87, 355–366 (2004).
9. López-Felices, B. et al. Farmers' profiles and attitudes towards the implementation of rainwater harvesting systems in intensive agriculture. Int. J. Agric. Sustain. 21 (2023).
10. van der Salm, C. et al. Minimising emissions to water bodies from NW European greenhouses; with focus on Dutch vegetable cultivation. Agric. Water Manag. 242, 106398 (2020).
11. Yazdi, M.N. et al. Specialty crop retention reservoir performance and design considerations to secure quality water and mitigate non-point source runoff. J. Clean Prod. 321, 128925 (2021).
12. Baudoin, W. et al. Good Agricultural Practices for greenhouse vegetable crops. Principles for Mediterranean climate areas. FAO PLANT PRODUCTION AND PROTECTION PAPER 217 (2013).

ARTICLE IN PRESS

ARTICLE IN PRESS

13. Incrocci, L. et al. Irrigation management of European greenhouse vegetable crops. Agric. Water Manag. 242 (2020).
14. Allen, R.G. et al. Crop evapotranspiration (guidelines for computing crop water requirements). FAO Irrig. Drain. Pap. No. 56, 1–333 (1998).
15. Fernández, M.D. et al. Measurement and estimation of plastic greenhouse reference evapotranspiration in a Mediterranean climate. Irrig. Sci. 28, 497–509 (2010).
16. Goddek, S. et al. How greenhouse horticulture in arid regions can contribute to climate-resilient and sustainable food security. Glob. Food Secur. 100701 (2023).
17. Zou, H. et al. Solar-driven scalable hygroscopic gel for recycling water from passive plant transpiration and soil evaporation. Nat Water. 2, 663–673 (2024).
18. la Cecilia, D. et al. Pixel-based mapping of open field and protected agriculture using constrained Sentinel-2 data. ISPRS Open J. Photogramm. Remote Sens. 8, 100033 (2023).
19. Tong, X. et al. Global area boom for greenhouse cultivation revealed by satellite mapping. Nat. Food 5, 513–523 (2024).
20. Aglagal, C. et al. Toward sustainable agricultural water management in an agribusiness system: a case study of the Chtouka plain, Morocco. Euro-Mediterr. J. Environ. Integr., (2025).
21. Azarnivand, A. et al. Modeling hydrological impacts of afforestation on intermittent stream. Sci. Total Environ. 728, 138748 (2020).
22. Azarnivand A. et al. Simulated response of an intermittent stream to rainfall frequency patterns. Hydrol. Process. 34, 615–632 (2020).
23. Daneshmand, H. et al. Water and salt balance modelling of intermittent catchments using a physically-based integrated model. J. Hydrol. 568, 1017-1030 (2019).

ARTICLE IN PRESS

ARTICLE IN PRESS

24. Gatto, B. et al. Quantifying groundwater recharge in the Venetian high plain between the Brenta and Piave Rivers through integrated surface–subsurface hydrological modeling. J. Hydrol. Reg. Stud. 50, 101550 (2023).
25. la Cecilia, D. et al. From weather data to water fluxes simulation in Mediterranean greenhouses through a combined climate and hydrological modelling approach. Agric. Water Manag. 311, 109386 (2025).
26. Camporese, M. et al. Surface–subsurface flow modeling with path-based runoff routing, boundary condition-based coupling, and assimilation of multisource observation data. Water Resour. Res. 46, W02512 (2010).
27. la Cecilia, D. & Despini, F. Protected agriculture mapping at continental scale for highlighting hotspots of altered hydrological processes. Remote Sens. Appl.: Soc. Environ. 37, 101509 (2025).
28. Rouse, J.W. et al. Monitoring vegetation systems in the great plains with ERTS. S.C. Freden, E.P. Mercanti, M. Becker (Eds.), Third Earth Resources Technology Satellite–1 symposium.Volume I: Technical Presentations, NASA SP-351, NASA, Washington, D.C., pp. 309-317 (1974).
29. Scanlon, B.R. et al. Global water resources and the role of groundwater in a resilient water future. Nat Rev Earth Environ 4, 87–101 (2023).
30. Campra, P. & Millstein, D. Mesoscale climatic simulation of surface air temperature cooling by highly reflective greenhouses in SE Spain. Environ. Sci. Technol. 47, 12284-12290 (2013).
31. Ali, E. et al. Cross-Chapter Paper 4: Mediterranean Region. In: Climate Change 2022: Impacts, Adaptation and Vulnerability. Contribution of Working Group II to the Sixth Assessment

ARTICLE IN PRESS

ARTICLE IN PRESS

Report of the Intergovernmental Panel on Climate Change. Cambridge University Press, 2233–2272 (2022).

32. European Environment Agency. European Climate Risk Assessment Executive Summary. EEA Report 01/2024. Luxembourg: Publications Office of the European Union (2024).
33. MASE. Piano Nazionale di Adattamento ai Cambiamenti Climatici. Rome: MASE.https://www.mase.gov.it/portale/piano-nazionale-di-adattamento-ai-cambiamenti-climatici-pnacc (2023).
34. Blum, A.G. et al. Causal effect of impervious cover on annual flood magnitude for the United States. Geophys. Res. Lett. 47, e2019GL086480 (2020).
35. Hersbach, H. et al. ERA5 hourly data on single levels from 1940 to present. Copernicus Climate Change Service (C3S) Climate Data Store (CDS) (2023) (Accessed 12 May 2024).
36. Tarquini S. et al. TINITALY, a digital elevation model of Italy with a 10 meters cell size (Version 1.1). Istituto Nazionale di Geofisica e Vulcanologia (2024).
37. la Cecilia, D. & Camporese, M. Resolving streamflow diel fluctuations in a small agricultural catchment with an integrated surface-subsurface hydrological model. Hydrol. Process. 36, e14768 (2022).
38. la Cecilia, D. et al. Data for: From weather data to water fluxes simulation in Mediterranean greenhouses through a combined climate and hydrological modelling approach. 10.25430/researchdata.cab.unipd.it.00001493 (2025).
39. Engelund, F. Hydraulic resistance of alluvial streams. J. Hydraul. Div., Am. Soc. Civ. Eng. (1966)

ARTICLE IN PRESS

ARTICLE IN PRESS

40. Camporese, M. et al. Catchment-scale Richards equation-based modeling of evapotranspiration via boundary condition switching and root water uptake schemes. Water Resour. Res. 51, 5756–5771 (2015).

41. Camporese, M. et al. Computing groundwater recharge and saturated storage dynamics: A Richards equation-based recipe. Water Resour. Res. 61, e2025WR039997 (2025).

42. Batjes, N.H. et al. Providing quality-assessed and standardised soil data to support global mapping and modelling (WoSIS snapshot 2023). Earth Syst. Sci. Data Discuss 16, 4735–4765 (2024).

43. Carsel, R.F. & Parrish, R.S. Developing joint probability distributions of soil water retention. Water Resour. Res. 24, 755–769 (1988).

44. van Genuchten, M.T. A closed form equation for predicting the hydraulic conductivity of unsaturated soils. Soil Sci. Soc. Am. J. 44, 892–898 (1980).

45. la Cecilia, D. et al. Data for: Expansion of greenhouses alters water use and underscores the need to balance food and water security in Mediterranean catchments. 10.25430/researchdata.cab.unipd.it.00001710 (2026).

46. Gupta, H.V. et al. Decomposition of the mean squared error and NSE performance criteria: implications for improving hydrological modelling. J. Hydrol. 377, 80–91 (2009).

47. Raffa, M. et al. Very High Resolution Projections over Italy under different CMIP5 IPCC scenarios. Sci Data 10, 238 (2023).

48. Coppola, E., et al. A first-of-its-kind multi-model convection permitting ensemble for investigating convective phenomena over Europe and the Mediterranean. Clim Dyn 55, 3–34 (2020).

ARTICLE IN PRESS

ARTICLE IN PRESS

Acknowledgements

This research is part of the MSCA-PF project REWATERING and received funding from the European Union's Horizon Europe research and innovation programme under the Marie Skłodowska-Curie grant agreement No. 101062255.

Author contributions

D.L.C.: conceptualization, investigation, methodology, validation, data curation, visualization, writing—first draft, writing—editing, funding acquisition.

C.P.: software, writing—editing.

P.M.: climate change data provision, writing-editing.

M.C.: conceptualization, methodology, software, resources, writing—editing, funding acquisition.

ARTICLE IN PRESS

ARTICLE IN PRESS

Figure 1|Schematic of altered hydrological processes in soil-bound greenhouse agriculture (left) compared to open-field agriculture (right). The boxplots represent the variability of water fluxes, with colours that match the corresponding hydrologic variables. Crop evapotranspiration is larger in open-field conditions and more variable than under controlled greenhouse settings, reflecting changes in weather conditions. Infiltration is generally lower and less variable in greenhouse conditions, because it is decoupled from rainfall. Runoff becomes larger in greenhouses because rainfall is quickly channelled to adjacent drainage canals.

Figure 2|Study area. a Overview of the *Piana del Sele* (Maps Data: Google Earth, SIO, NOAA, US Navy, NGA, GEBCO / Landsat, Copernicus) and **b-e** temporal evolution of the land use in the area, characterized by an increase in plastic greenhouses (Maps data: Landsat).

ARTICLE IN PRESS

Figure 3|Illustration of the modelling framework and the land use scenarios evaluated. Scheme of the developed workflow with the steps taken for preprocessing meteorological data and satellite data to generate the hydrological boundary conditions, the land cover and the corresponding hydraulic properties. The scheme visualizes how CATHY can limit evapotranspiration based on the Feddes model and irrigation supply using the developed routine. Finally, the maps display the land use scenarios evaluated.

Figure 4|Streamflow simulation for different land use and climate scenarios. a Simulated streamflow for the three land use configurations under the short-term scenario: i) the

ARTICLE IN PRESS

reference, ii) with winter crops (past scenario, before greenhouse development), and iii) with greenhouses over the whole agricultural area (hypothetical future scenario with greenhouses completely covering the catchment). **b** Cumulative overland flow volume for the same three land uses under the long-term scenario.

Figure 5|Groundwater storage depth for different land use and climate scenarios. a Time series of calculated groundwater storage depth for the three land use configurations in the short-term scenario: in the reference, in the lack of greenhouses (replaced with winter crops), and in the presence of greenhouses over the whole agricultural area. **b** Time series of simulated groundwater storage depth over time in the same three land use configurations under the long-term scenario. The dashed lines represent the long-term trend of the groundwater storage depth for the three land use scenarios.

ARTICLE IN PRESS

Figure 6|Irrigation water demand versus supply. Cumulative **a** irrigation water demand and **b** supply for the reference scenario, the open field-only scenario, and the greenhouse-only scenario. Note the log-scale y-axis in panel **b**, to better highlight the much smaller irrigation supply in the open field-only scenario.

Figure 7|Long-term trends in irrigation water supply. Left panels: irrigation water supply as a function of total rainfall for open-field crops aggregated by season and averaged by decade in the reference scenario (circles) and in the open field-only scenario (triangles). Right panels:

ARTICLE IN PRESS

irrigation water supply as a function of total rainfall for greenhouses aggregated by season and averaged by decade in the reference scenario (circles) and in greenhouse-only scenario (squares). The solid black lines show linear regressions for the reference scenario, while the black dashed lines indicate linear regression for the open field-only (a) and greenhouse-only (b) scenarios.

Figure 8|Evaluation of streamflow model performance. Time series of measured streamflow and simulated streamflow with the CATHY model corrected for the baseflow. The top graph with reversed y-axis reports the rainfall rate (P).

ARTICLE IN PRESS

ARTICLE IN PRESS

Table *1* | Aggregated land uses, corresponding areas in km^2, prescribed root depths, and Feddes model parameters.

Aggregated land cover	ID	Area (Km^2)	Root depth (m)	Ψ_{wp} (m)	Ψ_d (m)	Ψ_{an} (m)	Ψ_s (m)
Plastic greenhouses	1	3.68	0.3	-150	-4	-0.5	0
Storage facilities	2	0.01	0.001	-	-	-	-
Open-field agriculture (with insect net)	3	0.07	2.0	-150	-4	-0.5	0
Open-field agriculture	4	2.90	0.5	-150	-4	-0.5	0
Residential	5	0.07	0.001	-	-	-	-
Residential and infrastructures with vegetation	6	3.05	0.5	-	-	-	-

ARTICLE IN PRESS

ARTICLE IN PRESS

Table 2|Soil properties and hydraulic parameters for the reference simulation. The specific storage coefficient was set to 1.0×10^{-3} m^{-1} for all simulations.

Land cover	Depth (cm)	Horizontal K_{sat}[1] ($m\ s^{-1}$)	Vertical K_{sat}[1] ($m\ s^{-1}$)	ϕ[2] (-)	θ_r[3] (-)	n[4] (-)	α[4] (m^{-1})
Greenhouse	0-2	2.89×10^{-6}	1.00×10^{-10}	0.43	0.08	1.56	3.59
Land cover ID from 2 to 6 in Table 1	0-2	2.89×10^{-6}	2.89×10^{-6}	0.43	0.08	1.56	3.59
Greenhouse	170-200	5.55×10^{-8}	5.55×10^{-8}	0.36	0.07	1.09	2.00
Land cover ID from 2 to 6 in Table 1	170-200	2.89×10^{-6}	5.55×10^{-8}	0.36	0.07	1.09	2.00

[1] Saturated hydraulic conductivity, [2] Porosity, [3] Residual water content, [4] van Genuchten retention curve parameters[43].

ARTICLE IN PRESS

Editorial summary:
Greenhouse expansion reshapes regional water balances—reducing evapotranspiration, shifting irrigation needs, and altering streamflow and groundwater, as shown by an integrated climate, remote sensing, and hydrological modeling framework.

Peer review information:

Communications Earth & Environment thanks the anonymous reviewers for their contribution to the peer review of this work. Primary Handling Editors: Martina Grecequet and Srinivas Rallapalli. A peer review file is available

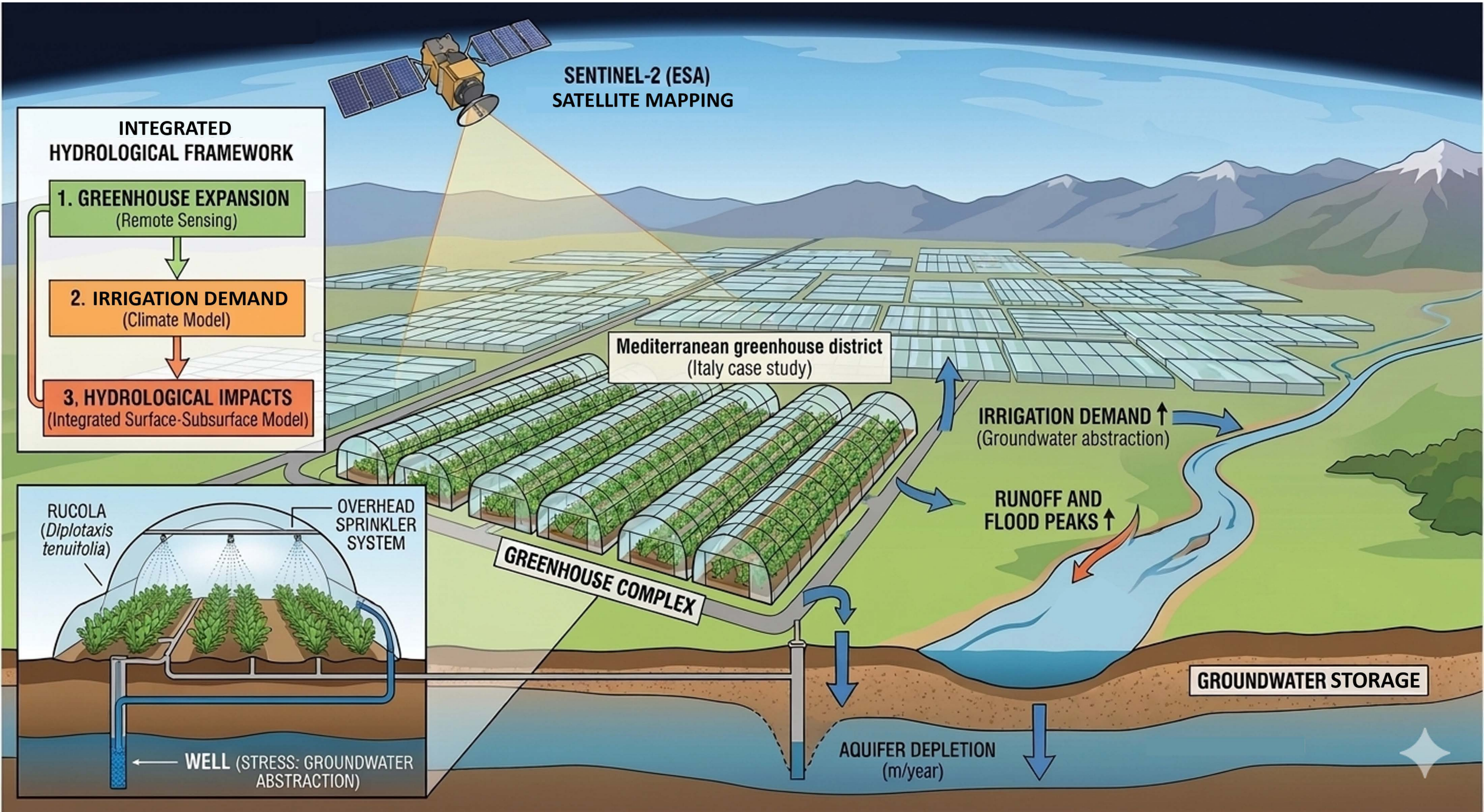
SENTINEL-2 (ESA)
SATELLITE MAPPING
INTEGRATED
HYDROLOGICAL FRAMEWORK
1. GREENHOUSE EXPANSION
(Remote Sensing)
2. IRRIGATION DEMAND
(Climate Model)
3, HYDROLOGICAL IMPACTS
(Integrated Surface-Subsurface Model)
Mediterranean greenhouse district
(Italy case study)
IRRIGATION DEMAND ↑
(Groundwater abstraction)
RUNOFF AND
FLOOD PEAKS ↑
GREENHOUSE COMPLEX
RUCOLA
(Diplotaxis
tenuifolia)
OVERHEAD
SPRINKLER
SYSTEM
WELL (STRESS: GROUNDWATER
ABSTRACTION)
AQUIFER DEPLETION
(m/year)
GROUNDWATER STORAGE

ARTICLE IN PRESS

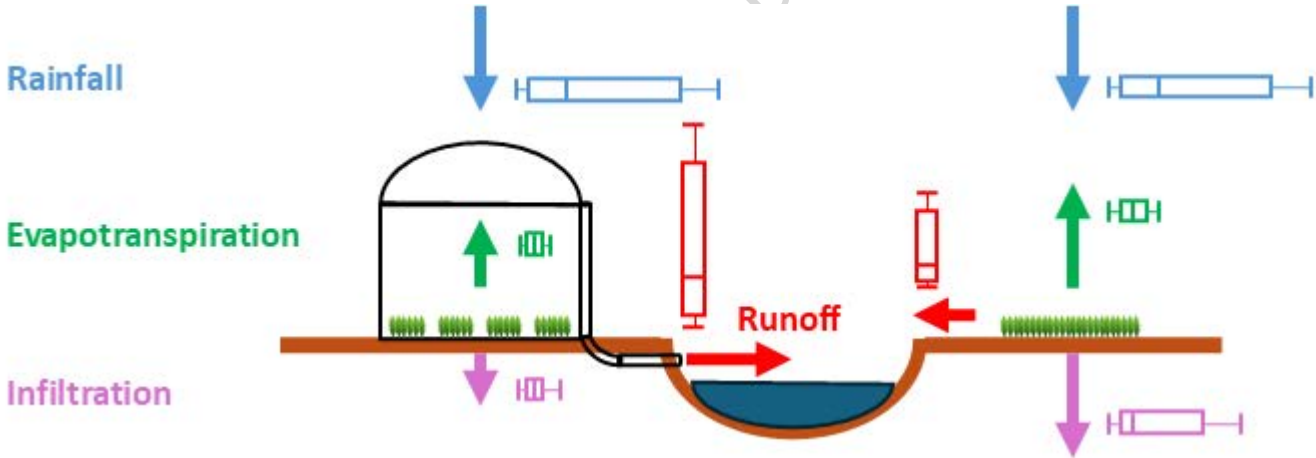

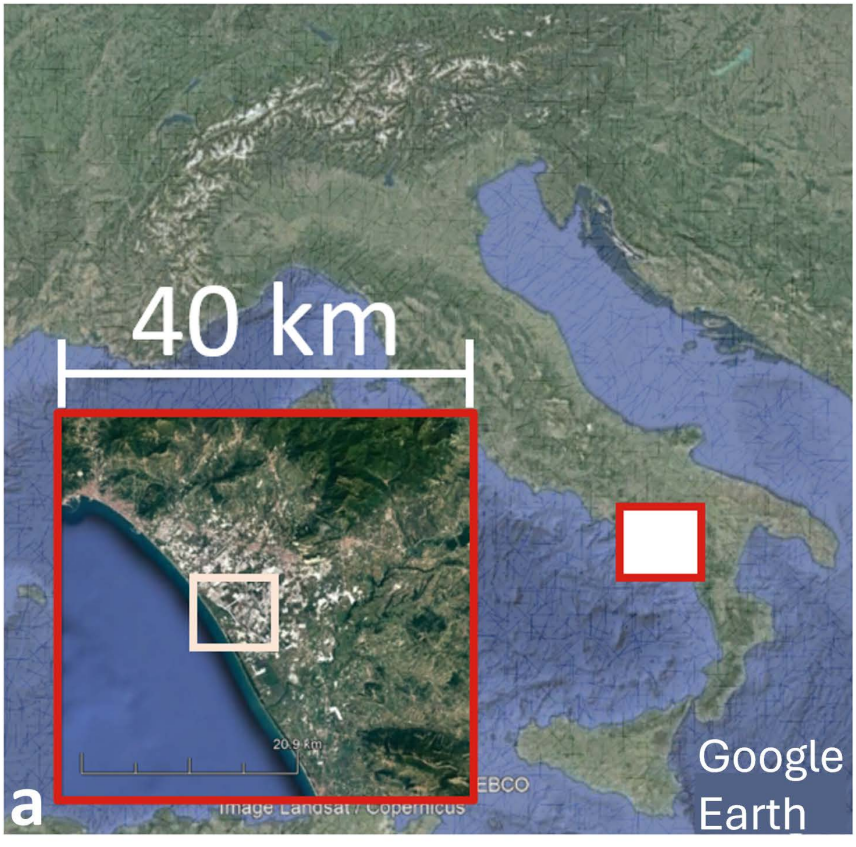

1984 – Landsat 5

1998 – Landsat 5

2011 – Landsat 5

2024 – Sentinel 2

		Greenhouses	Open Fields
Preprocessing for boundary conditions	ET_0 (mm h^{-1})	Outdoor weather data → greenhouse climate model	Outdoor weather data → Penman-Monteith equation
	K_C (-)	Local practice (K_C^G=0 in June and July, K_C^G=1 otherwise)	Remote sensing (K_C^{OF}=0 when NDVI<0.4, K_C^{OF}=1 otherwise)
	ET_C (mm h^{-1})	$ET_C^G = ET_0^G \times K_C^G$	$ET_C^{OF} = ET_0^{OF} \times K_C^{OF}$
	Irrigation demand (mm h^{-1})	Daily ET_C^G applied over 3 hours	Daily ET_C^{OF} applied over 1 hour
CATHY	Actual ET_C (mm h^{-1})	Feddes model $ET_C \times \propto(\psi)$ 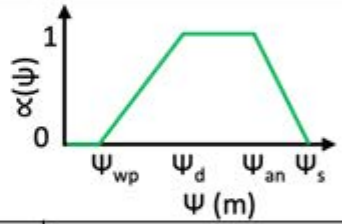	
	Irrigation supply (mm h^{-1})	Source term in the third soil layer from top	Atmospheric BCs with threshold on water saturation (S_w=0.35)

Land Use scenarios

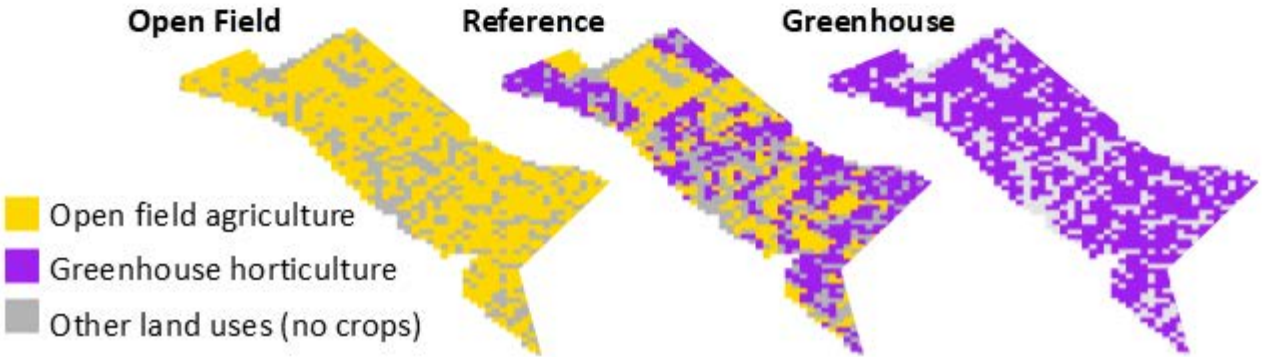

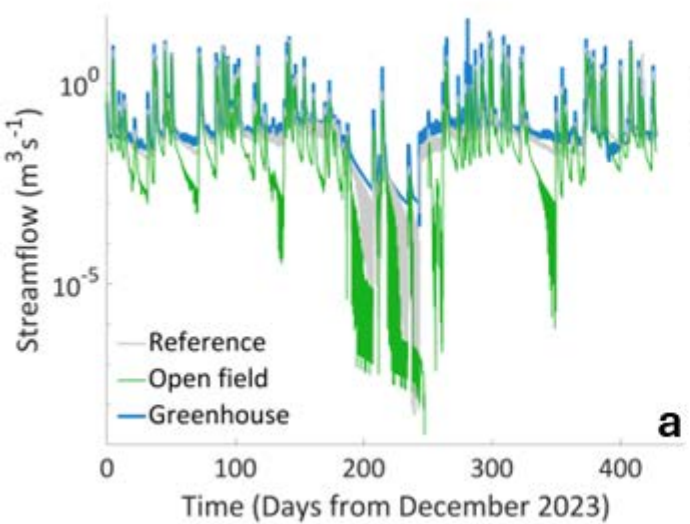
Streamflow ($m^3 s^{-1}$)
10^0
10^{-5}
Reference
Open field
Greenhouse
a
0
100
200
300
400
Time (Days from December 2023)

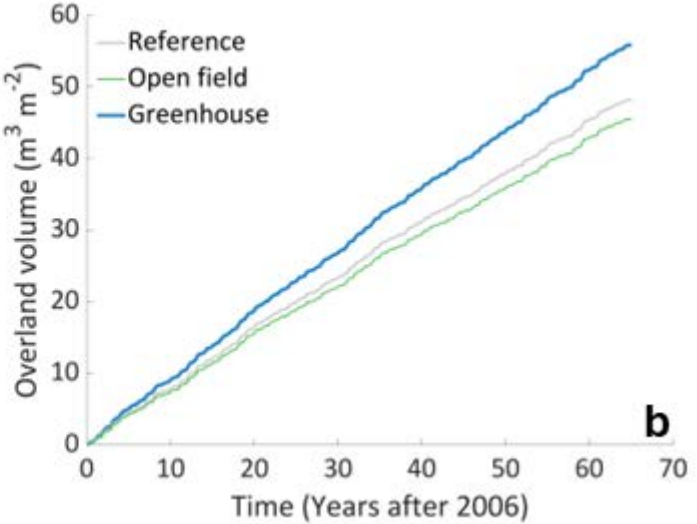
Overland volume ($m^3 m^{-2}$)
Reference
Open field
Greenhouse
b
0
10
20
30
40
50
60
70
Time (Years after 2006)

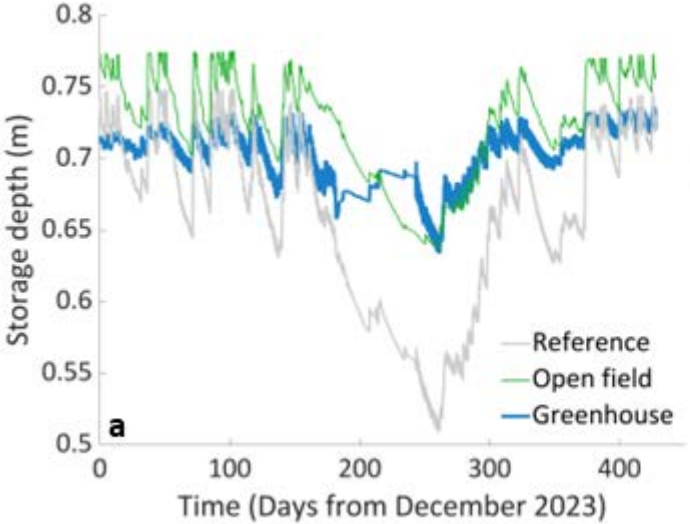
0.8
0.75
0.7
0.65
0.6
0.55
0.5
Storage depth (m)
Reference
Open field
Greenhouse
a
0
100
200
300
400
Time (Days from December 2023)

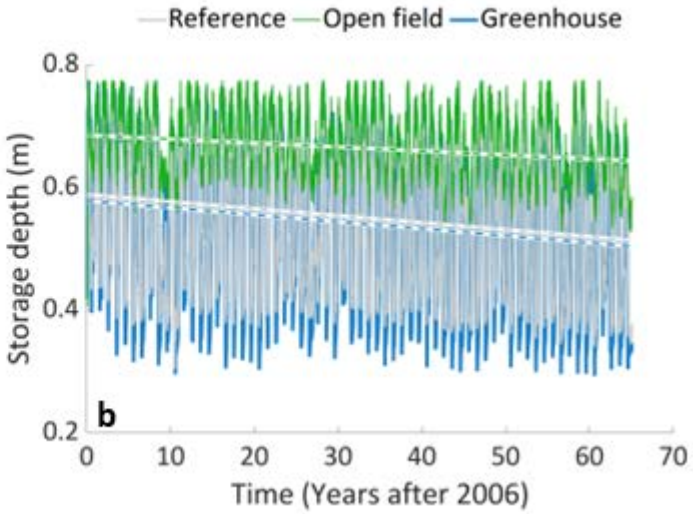
Reference
Open field
Greenhouse
0.8
0.6
0.4
0.2
Storage depth (m)
b
0
10
20
30
40
50
60
70
Time (Years after 2006)

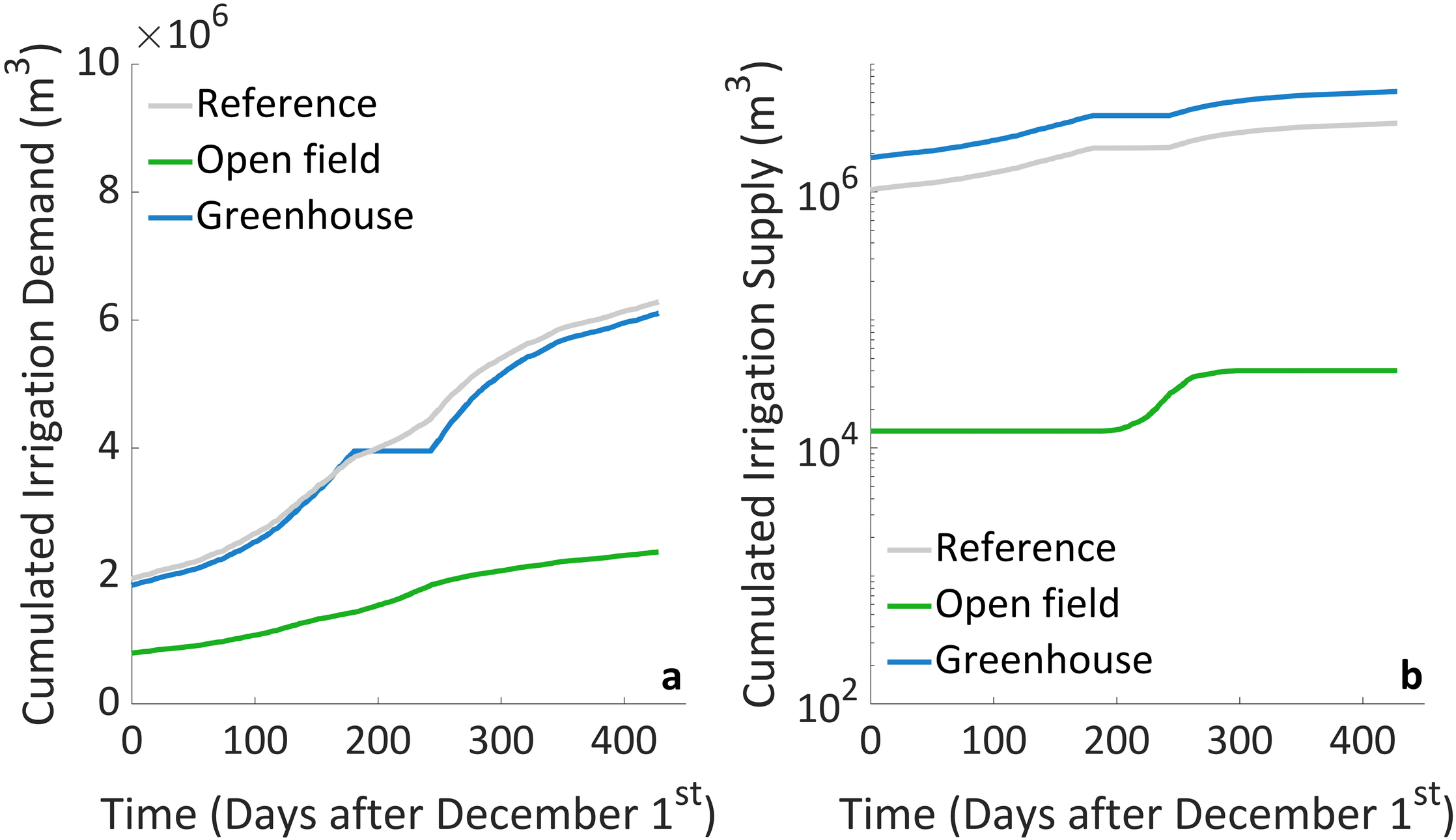
×10^6
Cumulated Irrigation Demand (m^3)
10
8
6
4
2
0
Reference
Open field
Greenhouse
a
0
100
200
300
400
Time (Days after December 1st)
Cumulated Irrigation Supply (m^3)
10^6
10^4
10^2
Reference
Open field
Greenhouse
b
0
100
200
300
400
Time (Days after December 1st)

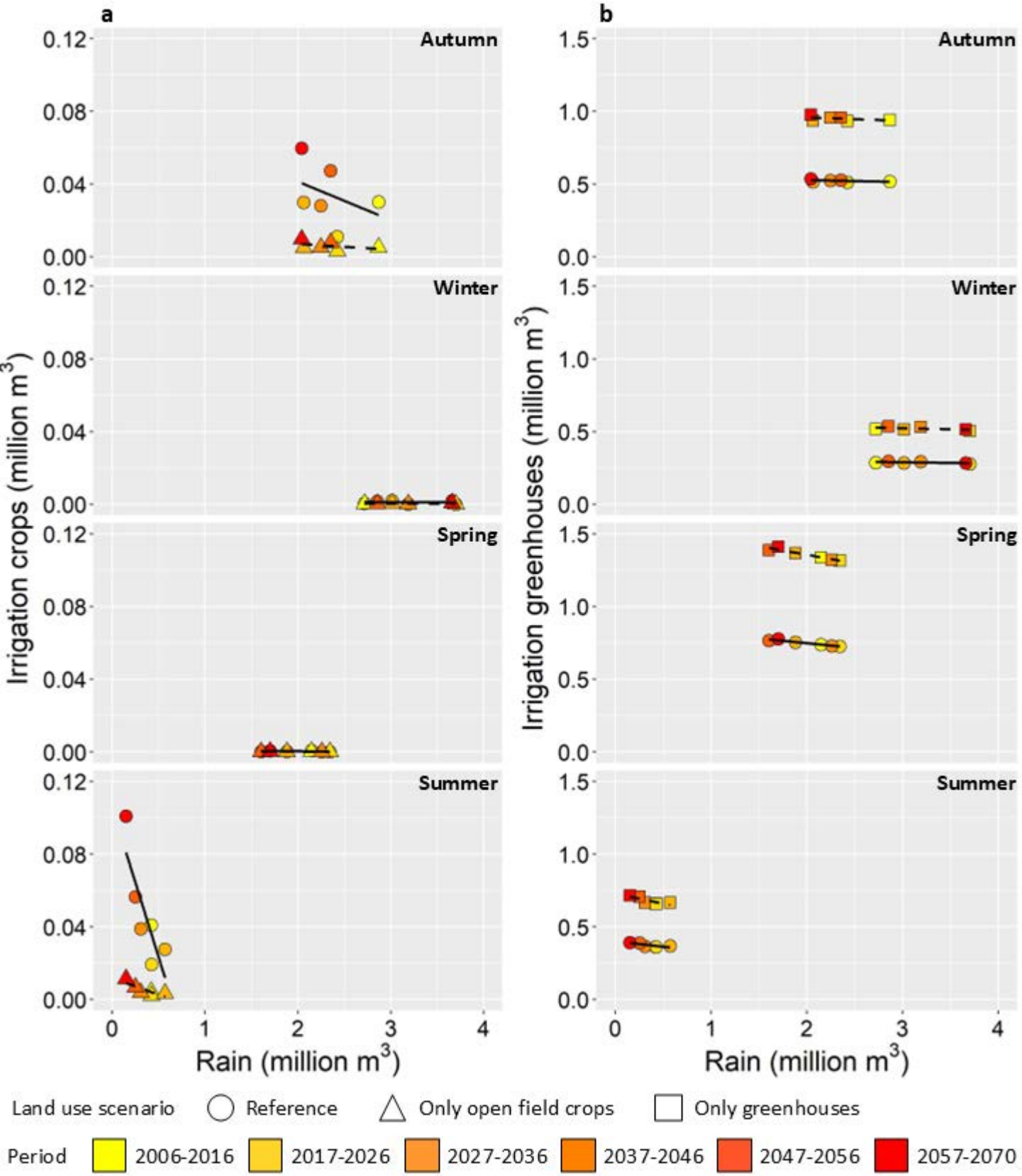
a
b
Autumn
Winter
Spring
Summer
Irrigation crops (million m3)
Irrigation greenhouses (million m3)
Rain (million m3)
Land use scenario
Reference
Only open field crops
Only greenhouses
Period
2006-2016
2017-2026
2027-2036
2037-2046
2047-2056
2057-2070

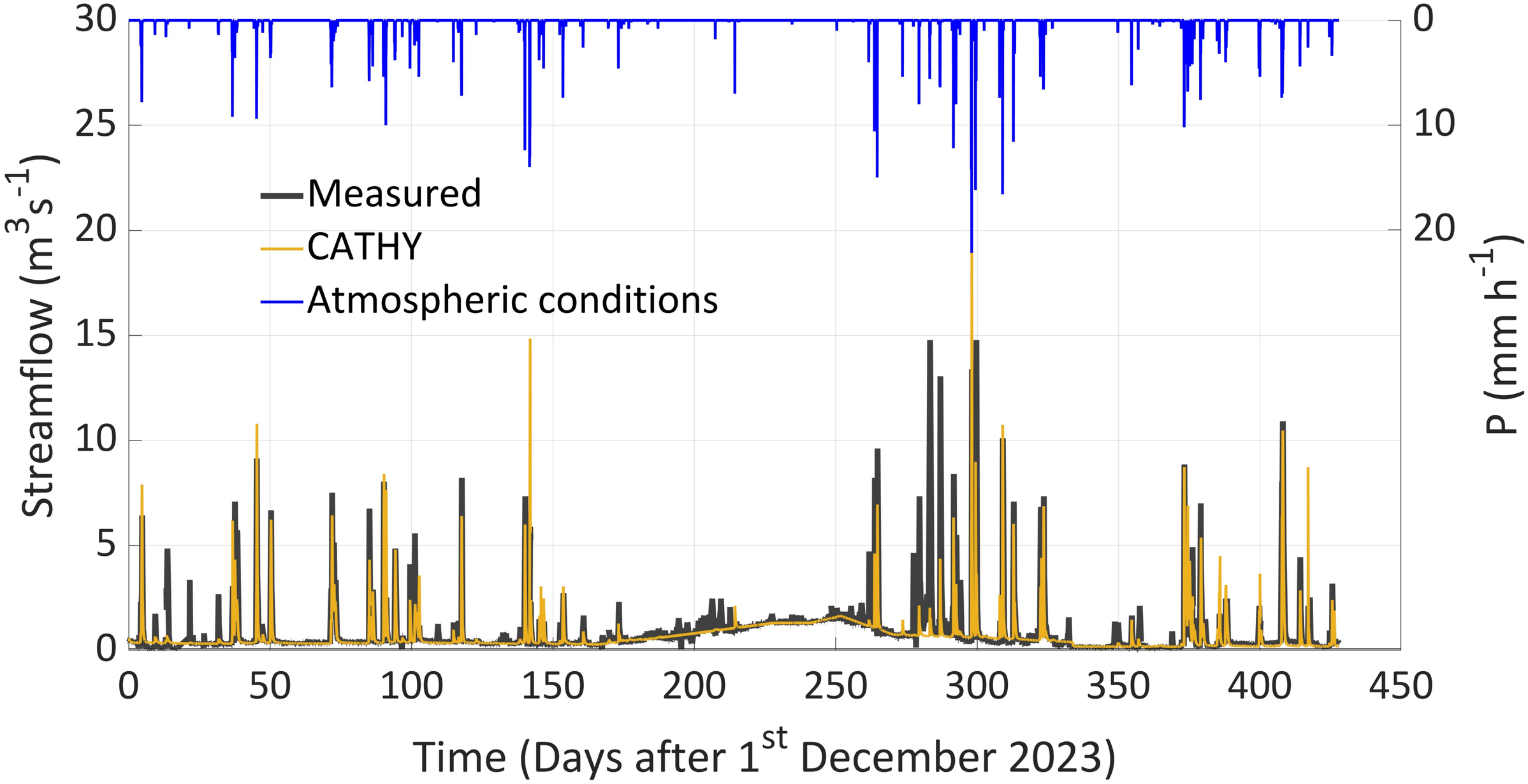
Measured
CATHY
Atmospheric conditions
Streamflow (m3s-1)
P (mm h-1)
Time (Days after 1st December 2023)
0
5
10
15
20
25
30
0
10
20
0
50
100
150
200
250
300
350
400
450